



Macrosegregation and microstructure dendritic array affecting the electrochemical behaviour of ternary Al–Cu–Si alloys

Wislei R. Osório^{a,b,*}, Daniel J. Moutinho^b, Leandro C. Peixoto^b, Ivaldo L. Ferreira^c, Amauri Garcia^b

^a School of Applied Sciences/FCA, University of Campinas, UNICAMP, Campus Limeira, 1300, Pedro Zaccaria St., Jd. Sta Luiza, 13484-350 Limeira, SP, Brazil

^b Department of Materials Engineering, University of Campinas, UNICAMP, P.O. Box 6122, 13083-970 Campinas, SP, Brazil

^c Department of Mechanical Engineering, Fluminense Federal University, Av. dos Trabalhadores, 420-27255-125 Volta Redonda, RJ, Brazil

ARTICLE INFO

Article history:

Received 28 March 2011

Received in revised form 8 July 2011

Accepted 8 July 2011

Available online 19 July 2011

Keywords:

Al–Cu–Si alloys

Macroseggregation

Microstructure

Electrochemical impedance spectroscopy

ABSTRACT

The aim of the present study is to evaluate the electrochemical corrosion behaviour of ternary as-cast Al–Cu–Si alloys. Electrochemical impedance spectroscopy (EIS), potentiodynamic anodic polarization techniques and an equivalent circuit analysis were used to evaluate the corrosion resistance in a 0.5 M NaCl solution at 25 °C. It was found that silicon and copper contents, which are affected by position in casting due to macrosegregation, and the dendrite arm spacing, can play an interdependent role on the corrosion behaviour. For the region with predominant Cu inverse segregation, i.e., close to the casting surface, the Cu content is the driving-force leading to a decrease in the corrosion resistance, but the favorable effect of the fineness of the dendritic array has also to be taken into account. However, from secondary dendrite arm spacings of about 15 μm up to coarser dendritic arrays, the Si particles seem to be the driving-forces related to the corrosion resistance and for these cases coarser microstructures were shown to improve the corrosion resistance.

© 2011 Elsevier Ltd. All rights reserved.

1. Introduction

Aluminum alloys have been widely used in the automotive and aerospace industries, in household appliances, electronic devices, etc., due to many favorable characteristics which includes high electrical and thermal conductivities, high specific strength, low density, high ductility, excellent castability, low cost, reasonable corrosion resistance, high strength-to-weight ratio and a relative balance of properties is attained using suitable heat treatments [1–7]. In particular, the automotive industry has increased recently the production of aluminum alloy castings for engine blocks and cylinder heads [7–9].

Copper is added to aluminum alloys to increase their strength, hardness, fatigue and creep resistances and machinability [10]. Quaresma et al. [11] reported that for similar secondary dendrite arm spacings an Al–15 wt.% Cu alloy was shown to have a higher ultimate tensile strength than an Al–4.5 wt.% Cu alloy. It has been reported that among the main aluminum-based alloys, Al–Cu alloys have the lowest negative potential of corrosion [10]. Copper generally reduces the resistance to general corrosion and, in specific compositions and material conditions, the stress corrosion

susceptibility [10]. Considering binary Al–Cu alloys, the Al₂Cu intermetallic phase has a cathodic behaviour with respect to the Al-rich matrix inducing considerable localized corrosion [12–15]. Osório et al. [12] reported that finer dendritic arrays provide a more extensive distribution of Al₂Cu particles along the finer interdendritic arms improving considerably the resulting corrosion resistance when compared with coarse microstructural arrangements.

Al–Si alloys have been used to replace a number of ferrous alloys in the automotive, transportation, and aerospace industries [16,17]. Their mechanical properties can have significant improvements by inducing structural modification in the normally occurring eutectic [18,19]. The mechanical properties of Al–Si alloys castings depend not only on their chemical composition but are also significantly affected by microstructural features such as the morphologies of the Al-rich α-phase and the eutectic Si particles [20,21]. Considering the corrosion resistance of Al–Si alloys, it has been reported that coarse dendritic structures tend to yield higher corrosion resistance than fine ones, and that this is associated with the more extensive distribution of the eutectic mixture which occurs for finer dendritic spacings and with the growth morphologies of the phases which constitute the interdendritic eutectic [18–22]. It has also been shown that the increase in the silicon content of these alloys provides a deleterious effect on the resulting corrosion resistance due to the corresponding increase in the eutectic volumetric fraction [22].

Al–Cu–Si alloys are also widely applied in both automotive and aerospace industries [23,24], mainly as light constructional

* Corresponding author at: Department of Materials Engineering, University of Campinas, UNICAMP, P.O. Box 6122, 13083-970 Campinas, SP, Brazil.
Tel.: +55 19 3521 3320; fax: +55 19 3289 3722.

E-mail address: wislei@fem.unicamp.br (W.R. Osório).

materials [25,26]. Al–Cu–Si alloys can also be used as thin-film interconnects in microelectronic devices [27]. Zhang et al. [28] classify copper as the most important alloying element in Al–Si casting alloys. It is added largely to increase the strength at low temperatures by solution treatment and at higher temperatures through the formation of compounds with iron, manganese, nickel, etc. [28]. However, as aforementioned, copper forms intermetallic Al_2Cu particles which tend to increase the susceptibility to localized (pitting) corrosion [12–15,29,30]. Considering the mechanical properties of Al–Cu–Si alloys, Zeren [24] highlighted the importance of using appropriate heat treatment techniques. He has also reported an increase in tensile strength and hardness with the increase in alloy copper content [24]. A recent review article by Sjölander and Seifeddine [31] presents a consistent synthesis on the influence of heat treatments on the resulting microstructure and mechanical properties of Al–Cu–Si alloys. However, the literature is scarce on studies dealing with the effects of microstructural features, particularly dendrite spacings, intermetallic particles and macrosegregation on the corrosion resistance of ternary Al–Cu–Si alloys. In previous studies [3,12,32], the effect of macrosegregation profiles on the corrosion resistance of a binary Al–Cu alloy has been investigated.

Normal and inverse macrosegregation profiles can also be found in ternary Al–Cu–Si alloy castings, as demonstrated by Ferreira et al. [33]. The present study aims to evaluate the combined effects of Si and Cu macrosegregation profiles, secondary dendrite arm spacing and intermetallic particles on the resulting electrochemical corrosion resistance of ternary Al–6 wt.% Cu–1 wt.% Si alloy castings. Samples were collected along the casting length and subjected to corrosion tests in a naturally stagnant 0.5 M NaCl solution at $25 (\pm 2)^\circ C$. The evaluation of the electrochemical corrosion resistance was based on results of an electrochemical impedance spectroscopy (EIS) technique, an equivalent circuit analysis and potentiodynamic polarization curves.

2. Experimental procedure

The solidification setup used to obtain a directionally solidified casting of an Al–6 wt.% Cu–1 wt.% Si alloy is shown in Fig. 1a. It was designed in such way that heat was extracted only through the water-cooled bottom, promoting vertical upward directional solidification (Fig. 1a). The stainless steel mold had an internal diameter of 50 mm, a height of 110 mm and a wall thickness of 3 mm. The side walls were covered with a layer of insulating alumina to minimize radial heat losses. The bottom part of the mold was closed with a thin (3 mm thick) carbon steel sheet, which physically separates the metal from the cooling fluid. Other details about the experimental procedure can also be found in a previous article [33].

Commercially pure grade (c.p.): Al (99.72 wt.%), Cu (99.92 wt.%) and Si (99.68 wt.%) were used to prepare the Al–6 wt.% Cu–1 wt.% Si alloy. The mean impurities detected were: Fe (0.25 wt.%), Pb (0.03 wt.%), Zn (0.01 wt.%) and Ni (0.01 wt.%), respectively, besides other elements found with concentrations less than 50 ppm.

Specimens were extracted from longitudinal sections, ground with silicon carbide papers up to 1200 mesh, polished and etched to reveal the microstructure (Keller's etchant: 1 mL of HF, 2.5 mL of HNO_3 , 1.5 mL of HCl and 95 mL of H_2O). Microstructural characterization was performed by an optical microscope associated with an image processing system Neophot 32 (Carl Zeiss, Esslingen, Germany) and a scanning electron microscope (SEM, Jeol JXA 840A). The segregation samples were underwent a Rigaku Rix 3100 X-ray fluorescence spectrometer to estimate their average concentration through an area of 100 mm² probe.

For corrosion tests, the working electrodes consisted of Al–Cu–Si alloy samples which were positioned at the glass corrosion cell kit,

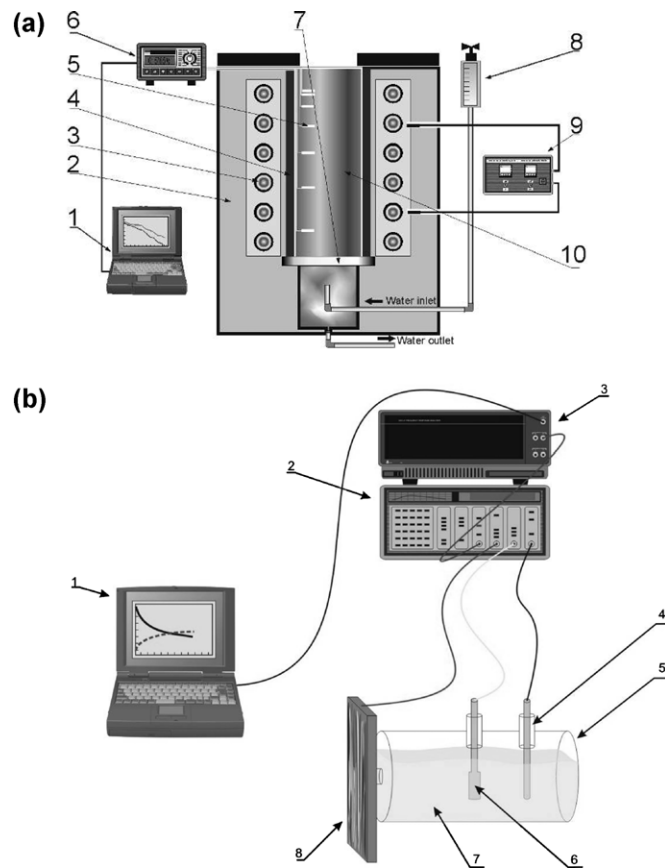


Fig. 1. (a) Schematic representation of the experimental solidification setup: (1) computer and data acquisition software; (2) insulating ceramic shielding; (3) electric heaters; (4) mold; (5) thermocouples; (6) data logger; (7) heat-extracting bottom; (8) water flow meter; (9) temperature controller; (10) casting and (b) a schematic representation of the experimental setup used for corrosion tests: (1) data acquisition system; (2) potentiostat; (3) frequency analyser; (4) reference electrode; (5) glass cell kit; (6) platinum counter-electrode; (7) 0.5 M NaCl solution; (8) Al–Cu–Si alloy work-electrode.

leaving a circular $1.0 (\pm 0.02) \text{ cm}^2$ metal surface in contact with a naturally aerated and stagnant 500 cm^3 of a 0.5 M NaCl solution at $25^\circ C$ and with $7.08 (\pm 0.8)$ pH. The samples were further carefully ground to a 600 grit SiC finish, followed by distilled water washing and air drying before electrochemical measurements.

EIS measurements began after an initial delay of 15 min for the sample to reach a steady-state condition. Although open-circuit potential measurements (OCP) have not been carried out, there were experimental evidences that after 15 min the potential steady-state condition had been reached. A potentiostat (EG & G Princeton Applied Research, model 273A) coupled to a frequency analyzer system (Solartron model 1250), a glass corrosion cell kit with a platinum counter-electrode and a saturated calomel reference electrode (SCE) were used to perform the EIS tests. The potential amplitude was set to 10 mV; peak-to-peak (AC signal) in open-circuit, with 5 points per decade and the frequency range was set from 100 mHz to 100 kHz.

Potentiodynamic tests were also carried out in a 0.5 M NaCl solution at $25^\circ C$ using a potentiostat at the same positions and immediately after the EIS measurements. These tests were conducted by stepping the potential at a scan rate of 0.1667 mV s^{-1} from -250 to $+250 \text{ mV}$ (SCE) at open-circuit. Using an automatic data acquisition system, the potentiodynamic polarization curves were plotted and both corrosion rate and potential were estimated by Tafel plots using both anodic and cathodic branches. Duplicate tests for both EIS and potentiodynamic polarization curves were

Download English Version:

<https://daneshyari.com/en/article/189215>

Download Persian Version:

<https://daneshyari.com/article/189215>

[Daneshyari.com](https://daneshyari.com)